detritus Multidisciplinary Journal for Waste Resources & Residues

CISA

SPATIAL MATHEMATICAL MODELING OF STATIC COMPOST PILES WITH HEAT RECOVERY

Geo Jacob [1,2,*], Frank Dienerowitz [1] and Nele Jaschke [2]

[1] Ernst-Abbe-Hochschule Jena, Department of SciTec, Jena, Thüringia, Germany
[2] Deutsche Biomasseforschungszentrum gemeinnützige GmbH (DBFZ), Department of Bioenergy Systems, Leipzig, Germany

Article Info:
Received:
26 February 2022
Revised:
3 July 2022
Accepted:
3 August 2022
Available online:
14 September 2022

Keywords:
Composting
Heat recovery
Mathematical modeling
Static compost pile
Heat transfer
Numerical simulation

ABSTRACT

Composting experiments with heat recovery reveal spatial non-uniformity in parameters such as temperature, oxygen concentration and substrate degradation. In order to recover heat from static compost piles via integrated heat exchanger there is the need to investigate the temperature distribution for placing the heat exchangers and the interaction between heat recovery, substrate degradation and oxygen concentration to ensure quality of composting process. This study introduces a spatial model to predict the variation in controlling parameters such as temperature, oxygen concentration, substrate degradation and airflow patterns in static compost piles with heat recovery using Finite element method (FEM) in COMSOL Multiphysics ® Version 5.3. The developed two-dimensional axisymmetric numerical model considers the compaction effects and is validated to real case pilot-scale compost pile experiments with passive aeration. Strong matching with the real case experiment was achieved. The spatial model demonstrated that the compaction effect is extremely important for realistic modeling because it affects airflow, temperature distribution, oxygen consumption and substrate degradation in a compost pile. Heat recovery did not disrupt the composting process. Case studies revealed strong influence of convective heat loss through the edges and a 10% improvement of heat recovery rate with ground insulation. The simulation indicates that an optimized placing of heat recovery pipes could increase the average heat extraction by 10-40%.

1. INTRODUCTION

Composting is an aerobic degradation process influenced by microbial and chemical reactions in which the controlling factors are temperature, oxygen content, moisture content, C: N ratio of the material, initial microbial community, aeration, degradation rate, porosity, density, water retention capability and pH of the material (Müller, 2017; Mason I. G., 2006; Hamelers, 2001; Haug, 1993; Malesani, et al., 2021). Heat energy utilization from the natural process of composting is both a sustainable waste management practice with compost as a final product and heat energy as a renewable energy source, thereby contributing to meet the goals of the Paris agreement (European Environment Agency, 2017; Schmidt-Baum, et al., 2020). In the mid 1970's, self-made scientist Jean Pain described a method to utilize the thermal energy for residential heating from pipes carrying water placed inside a compost pile (Müller, 2017; Zampieri, 2017). From then, different heat extraction methods were developed in which the heat exchangers are placed inside the biomass or by using an external heat exchanger that uses the exhaust air from composting process to recapture heat by condensation of water vapor (Müller, 2017; Schmidt-Baum, et al., 2020). In this study a mathematical model is developed for pilot scale compost piles with internal heat exchangers which were built as a part the project aimed at understanding the renewable energy potential of compost piles (Schmidt-Baum, et al., 2020).

Mathematical models serve as an aid to improve the system design and process for greater understanding and system optimization of composting systems (Hamelers, 2001; Vidriales-Escobar, et al., 2017). Also, mathematical modelling of the composting process is complex due to the large number of parameters to be considered for the model development (Hamelers, 2001; Rongfei, et al., 2017). A small glimpse on the literature indicates that many models were developed with different perspectives on heat recovery from compost piles (Mason I. G., 2006; Deipser, 2014; Nwanze & Clark, 2019; Mwape, et al., 2020). The main objectives by these studies were to understand the variations in parameters such as temperature, moisture content and oxygen distribution with time variations and spatial variations (Mason I. G., 2006; Lukyanova, 2012; Rongfei, et al.,

* Corresponding author:
Geo Jacob
email: ej.geo30@gmail.com

https://doi.org/10.31025/2611-4135/2022.15213

2017). In addition, some of these models were mostly developed for industrial scale processes (windrow composting) (Vidriales-Escobar, et al., 2017). Most of the mathematical models for in-vessel composting have assumed the composting process to take place uniformly in the vessel and under controlled operating conditions (Mason I. G., 2006). The outdoor pilot scale composting piles which are passively aerated are not under controlled operating conditions (Müller, 2017; Schmidt-Baum, et al., 2020). Experimental studies on composting in outdoor environment have indicated the spatial non-uniformity in parameters such as temperature, moisture content, gas concentrations, and degradation rates with variations in airflow when the composting process was performed (Müller, 2017; Deipser, 2014). Since the outdoor composting process is highly heterogeneous and dynamic, a spatial model can improve the understanding of the processes within the pile (Müller, 2017; Lukyanova, 2012).

A review of literature about (Table 1) previous spatial models was done considering the crucial parameters for the aim of the study. For pilot scale compost reactors with heat recovery and an internal heat exchanger, only the model by Zampieri studied heat recovery from compost piles but did not predict accurate results for more than two days (Zampieri, 2017). Forced aeration was considered in all models except in the model developed by Lukayanova which considered natural aeration, and which is the dominant factor in most of the outdoor windrow compost piles (Lukyanova, 2012; Müller, 2017). Compaction effects are also crucial for aeration, since the airflow in porous systems depend on density, porosity, and permeability (Lukyanova, 2012). However, the model from Lukyanova was validated based on indoor laboratory studies, which have different boundary conditions compared to outdoor compost piles. Thus, in this study a spatial model is developed considering the compaction effects and heat recovery from static outdoor compost piles with heat recovery.

1.1 Abbreviations

C: N	Carbon to Nitrogen Ratio [1]
S	Fraction of available substrate for degradation [kg/m³]
T	Compost pile temperature [K]
φ	Air filled porosity of the pile [1]
T_{amb}	Ambient air temperature [K]
$\vec{q}$	Volume flux of air [m/s]
k	Permeability [m²]
μ	Viscosity of air [Pa•s]
t	time [d]
O_2	Oxygen concentration in the pile [kg/m³]
P	Pressure [Pa]
K_T	Heat release rate [K/h]
K_{O_2}	Oxygen consumption rate [kg/m³•h]
K_S	Rate of substrate consumption [kg/m³•h]
g	Acceleration due to gravity [m/s²]
T_{air}	Temperature of air inside the compost pile [K]
h_i	Compaction factor [m]
T_{gro}	Ground temperature [K]
T_{pipe}	Pipe wall temperature [K]

2. MATERIALS AND METHODS

2.1 Experiment for model validation

Two experimental piles (55 m³) are considered in this study: one without a heat exchanger and another one with a heat exchanger inside the pile. The compost piles confined to cylindrical shape using wire meshes and conical form at top were constructed on 16th September 2018 before the autumn. The composting material consisted of a shredded mixture of garden waste including leaves, grass, twigs, soil, and straw. The size of the individual particles in the mixture varied from very fine to large parts that were bigger than 10 cm. The reference pile had only two sensors S1 and S2 while piles with heat exchangers had six temperature sensors. The data from the sensors placed in the compost pile without a heat exchanger were used for model validation. The detailed information of the experimental set-up, data collection methods and experimental results are listed in the reports by Müller and Schmidt-Baum et al. (Müller, 2017; Schmidt-Baum, et al., 2020; Jaschke & Schmidt-Baum, 2021).

2.2 Mathematical Model

2.2.1 Assumptions

In the model following assumptions of the composting process were made:

- The substrate is homogenous and is homogenously distributed in each portion of the pile.
- The compost pile is considered porous as a two-phase-system: The solid phase consists of degradable organic matter and water. The fluid phase is in the pores and consists of gases.
- The total volume and density of the compost pile is constant during the entire period of simulation.
- The thermal conductivity, heat capacity and diffusivity of the substrate does not change with time, is homogenous within the pile and does not change with heat extraction activity.
- The ambient pressure and ambient oxygen levels remained constant during the entire period of simulation.
- The changes of wind, precipitation and relative humidity are assumed null in this model.
- The changes in ground temperature are calculated based on experimental results and these values are used for all the different study variations (Schmidt-Baum, et al., 2020).
- The heat exchanger pipe wall boundary temperature is 35°C, considering that in the experiment the temperature of the water entering in the pipes is always at this temperature.

2.2.2 Governing Equations

The mathematical model is formulated based on the correction functions, biological reaction rates and the governing partial differential equations (PDE) for the main dependent variables considered in this model. The correction functions in the mathematical model control the changes in state variables with time and represent their interdependence. The biological reaction rate in a com-

TABLE 1: Overview of spatial modeling of composting systems.

Model	Geometry	Temperature	Oxygen consumption	Airflow	Substrate consumption	Moisture content	Heat exchanger	Compaction effects
Finger et al., 1976	Any	✓	✓	✗	✗	✗	✗	✗
Sidhu et al., 2006	1D, 2D	✓	✗	✗	✗	✗	✗	✗
Sidhu et al., 2007	2D	✓	✓	✗	✗	✗	✗	✗
Luangwilai & Sidhu, 2010	1D	✓	✓	✓	✗	✗	✗	✗
Luangwilai et al., 2010	2D	✓	✓	✓	✗	✓	✗	✗
Luangwilai et al., 2012	1D	✓	✓	✓	✗	✓	✗	✗
Zambra et al., 2011	2D	✓	✓	✗	✗	✓	✗	✗
Zambra et al., 2012	3D	✓	✓	✓	✓	✗	✗	✗
Lukyanova, 2012*	Any	✓	✓	✓	✓	✗	✗	✓
Luangwilai et al., 2018	1D	✓	✓	✓	✗	✓	✗	✗
Zampieri, 2017	2D	✓	✓	✓	✓	✓	✓	✓

✓ = considers the property, ✗ = does not consider property, * Selected model for further studies

posting process is influenced by temperature, oxygen content, moisture content, C:N ratio of the material, initial microbial community, aeration, degradation rate, porosity, density, water retention capability and pH of the material (Müller, 2017; Deipser, 2014; Nwanze & Clark, 2019). The model introduced in this study considers the dynamical variables which are temperature (T), oxygen (O_2), and substrate concentration (S) as these were the primary interest of the project/experimental investigation (see Introduction and Table 1) (Müller, 2017; Schmidt-Baum, et al., 2020). In addition to the dynamical variables T, O_2 and S, additional correction functions and parameters used in the different equations are listed in Table 2.

The temperature correction function determines temperature evolution based on growth of microorganisms (Hamelers, 2001; Haug, 1993). This function utilized by Lukayanova is simple and in agreement with model predictions and experimental data (Lukyanova, 2012). The temperature correction function was modified for this outdoor experiment considering the active temperature range for microbial growth which has the following form:

$$f(T) = \begin{cases} 0.0286 \cdot T, & 0 \le T \le 35 \\ 1, & 35 \le T \le 55 \\ 3.75 - 0.05 \cdot T, & 55 \le T \le 75 \\ 0, & T \ge 75 \end{cases} \quad (1)$$

Oxygen availability in the pile determines heat production (Hamelers, 2001). Lesser oxygen concentration leads to anaerobic conditions and thus finally to undesirable methane production (Müller, 2017). The oxygen correction function utilized in the model is of the Monod type. The normalized expression is used for an ambient concentration of oxygen, which has the following form:

$$g(O_2) = \frac{O_2}{H_{O_2} + O_2} \frac{H_{O_2} + O_2^{amb}}{O_2^{amb}}, g\left(O_2^{amb}\right) = 1 \quad (2)$$

Substrate degradation results in the temperature rise and oxygen consumption by microbes (Haug, 1993; Lukyanova, 2012). A Monod type expression was used as the substrate correction function. The normalized expression for substrate degradation could be expressed as:

$$h(S) = \frac{6}{5} \frac{S}{(S + S_0/5)}, h(S_0) = 1 \quad (3)$$

Here, S_0 is the initial substrate density available for decomposition.

Since heat release rate, oxygen consumption rate and substrate consumption rate are proportional, and they are connected by the stoichiometry of the reaction as:

$$K_T = K_T^* f(T) g(O_2) h(S);\ K_{O_2} = \\ = K_{O_2}^* f(T) g(O_2) h(S); K_S = K_S^* f(T) g(O_2) h(S) \quad (4)$$

Here, K_T^* is the maximum rate of heat release, $K_{O_2}^*$ is the maximum rate of oxygen consumption and K_S^* is the maximum rate of substrate consumption. f(T), g(O_2) and h(S) are the correction functions for temperature, oxygen, and substrate respectively.

The temperature of the compost pile is affected by ambient temperature, heat generation in the pile due to oxygen consumption and substrate degradation and heat loss due to air passing through the pile (Lukyanova, 2012). The net variation in the temperature in the compost pile could be expressed as:

$$\frac{\partial T}{\partial t} = D\nabla^2 T + K_T - \beta(T - T_{air}) \quad (5)$$

where $D\nabla^2 T$ represents the heat dissipation through the compost, K_T indicates the heat generation due to biological decomposition and $\beta(T-T_{air})$ indicates the heat loss to the air flowing through the compost pile.

The oxygen concentration in a pile depends on the availability of oxygen in the pile and the aeration (Müller, 2017). It is a function of degradation of the substrate and heat production in the compost pile. The net variation of oxygen concentration in the pile is described as:

$$\frac{\partial O_2}{\partial t} = d\nabla^2 O_2 + K_{O_2} - \nabla O_2 q \quad (6)$$

where $d\nabla^2 O_2$ indicates the diffusion of oxygen in the compost pile, K_{O_2} indicates the rate of oxygen consumption with variations in the temperature and substrate degrada-

TABLE 2: Parameter values implemented in the model.

Parameter	Units	Value	Description	Remarks
$C_{p,air}$	J/kg·K	1005	Heat capacity of air	(Lukyanova, 2012)
$C_{p,c}$	kg/m³	2600	Heat capacity of the composting material	Fitted
H_{O_2}	kg/m³	6.63e-2	Half saturation constant for oxygen	(Lukyanova, 2012)
$K^*_{O_2}(x)$	kg/m³-h	$\frac{Y_{O/S}K_S}{\varphi(x)}$	Maximum rate of oxygen consumption	(Lukyanova, 2012)
K^*_S	kg/m³ h	0.1	Maximum rate of substrate consumption	Fitted
$K^*_T(x)$	K/h	$\gamma\frac{Y_{H/S}K_S}{C_{p,c}\rho(x)}$	Maximum rate of heat release	Calculated
O_2^{amb}	kg/m³	$0.232\cdot\rho_{air}^{amb}$	Ambient oxygen concentration	(Haug, 1993)
P_{atm}	Pa	101325	Ambient atmospheric pressure	(Hamelers, 2001)
S_0	kg/m³	$0.400\cdot\rho_0$	Initial Substrate density	(Schmidt-Baum, et al., 2020)
T_{ini}	K	283	Initial compost pile temperature	(Jaschke & Schmidt-Baum, 2021)
U_g	W/m²-K	0.0056	Ground heat transfer coefficient considering small contact resistance	(Schmidt-Baum, et al., 2020)
U_w	W/m²-K	0.1944	Overall heat transfer coefficient	Calculated
$Y_{H/S}$	J/kg	1.91e7	Stoichiometric coefficient, that determines the amount of energy released from oxidation of a kg of substrate	(Liang, et al., 2004)
$Y_{O/S}$	kg/kg	1.37	Stoichiometric coefficient, that determines the amount of oxygen needed to oxidise a kg of substrate	(Lukyanova, 2012)
d_S	m²/h	1e-6	Diffusion coefficient of substrate added to improve numerical stability	(Lukyanova, 2012)
d_{air}	m²/h	0.0684·0.5	Thermal diffusion coefficient of air filling the porous surface	(Lukyanova, 2012)
f_g	1	0.5	Factor for heat loss calculation according to DIN-4108-6	(Schmidt-Baum, et al., 2020)
ρ_0	kg/m³	550	Initial compost pile bulk density	Fitted
ρ_{air}^{amb}	kg/m³	1.225	Ambient air density	Standard
φ_0	%	50	Air filled porosity of the pile	Fitted
a	1/m	$\frac{A}{V}$	Interfacial area available for heat transfer	Calculated
C	1/m²	1.03e8	Kozeny-Carman constant	(Yu, 2007)
D	m²/h	0.0004	Thermal diffusivity of the composting material	(Yu, 2007)
α	1/h	$\frac{aU_w}{\varphi_0 C_{p,air}\rho_{air}^{amb}}$	Coefficient characterizing rate of heating of air molecules in the compost	Calculated
β	1/h	$\frac{aU_w}{C_{p,c}\rho_0}$	Coefficient characterizing rate of cooling of compost transferring heat to air	Calculated
d	m²/h	0.0576·0.5	Diffusion coefficient for oxygen in the air filling the porous surface	(Lukyanova, 2012)
γ	1	0.25	Fraction of the total energy derived from biological decomposition of the substrate	Fitted
g	m/s²	9.8	Acceleration due to gravity	(Haug, 1993)

tion and $\nabla O_2\vec{q}$ controls the distribution of oxygen in the pile.

The amount of substrate decreases due to consumption. Since no substrate is further added, it decreases from the initial amount as a function of temperature and oxygen availability. The net degradation of the substrate could be described as:

$$\frac{\partial S}{\partial t} = d_S\nabla^2 S + K_S \tag{7}$$

where $d_S\nabla^2 S$ is the diffusion term added to the substrate to ensure numerical stability of the model. K_S indicates the degradation of the substrate due to oxygen concentration and temperature in the pile.

The air entering the pile absorbs the heat produced in the pile (Lukyanova, 2012). Therefore, it is important to incorporate the ventilation of the pile as an important parameter in controlling the process temperature. The variation in the temperature of the air entering the pile could be described by:

$$\frac{\partial T_{air}}{\partial t} = d_{air}\nabla^2 T_{air} + \alpha(T - T_{air}) - \nabla T_{air} q \tag{8}$$

where $d_{air}\nabla^2 T_{air}$ indicates the diffusion of the air molecules in the compost matrix, $\alpha(T-T_{air})$ indicates the heating of the air in the pores as it travels through different parts of the compost pile and $\nabla T_{air}\vec{q}$ indicates distribution of air in the compost pile. It also helps in heating other parts of the compost pile that have lower temperature as compared to the air temperature in the pores.

The airflow in the compost piles is formulated based on Darcy's law of fluid flow through porous media and considering the buoyancy effects on air molecules with increased temperature (Lukyanova, 2012). In the case of passive aeration, the Boussinesq approximation assumes the flow to be incompressible and the mathematical model can be completed with the continuity equation. The expression for airflow through the porous media is formulated as:

$$\vec{q} = \frac{k}{\mu}\left(\nabla P - \rho_{air}^{amb} g\varphi\left(1 - \frac{T_{amb}}{T}\right)\vec{e}_z\right) \quad (9)$$

$$\nabla \cdot \vec{q} = 0 \quad (10)$$

where $\vec{e_z}$ is a unit vector pointing upwards. Thus, when T> T_{amb}, the airflow will be in the upward direction and when T< T_{amb}, the airflow will be in the downward direction.

The compaction effects are incorporated in the model from the expressions from (Das & Keener, 1997). It is incorporated by considering the parameters to be varying as a function of depth y. The equations for compaction factor, porosity, permeability and bulk density are further modified from the parameter values from the experiment (Table 2). The expression for compaction factor is:

$$h_i(y) = 0.604 + 0.396 \cdot \exp\left(-\frac{0.105\rho_0(0.5-y)g}{1000}\right) \quad (11)$$

The variation of air-filled porosity as a function of depth considering the compaction effects is:

$$\varphi(y) = \frac{1}{h_i(y)}(\varphi_0 - 1) + 1 \quad (12)$$

The permeability of the compost matrix is modelled by the Kozeny-Carman model. This relates the value of permeability to the air-filled porosity:

$$k(y) = \frac{\varphi(y)^3}{C\left(1-\varphi(y)\right)^2} \quad (13)$$

where, C is the Kozeny-Carman constant. Thus, porosity and permeability vary in the pile from top to bottom. The variation in density with depth after considering the density changes after compaction of the pile could be expressed as:

$$\rho(y) = \frac{\rho_0}{h_i(y)} \quad (14)$$

2.2.3 Geometry

The axisymmetric distribution of state variables was shown by Müller and this geometric condition was chosen to reduce the computational effort and the complexity of the problem (Figure 1) (Müller, 2017). Also, this approach is chosen for sensor positions in the real case experiment. The probes (S1, S2, S3, S4) were placed in the geometry to identify the variations in dependent variables, namely: temperature, oxygen concentration, substrate degradation and airflow between the pipes. The heat exchanger setup consists of circular pipes of 0.032 m diameter, placed concentrically in the pile. This spiral arrangement of the heat exchangers was chosen to simplify the computation.

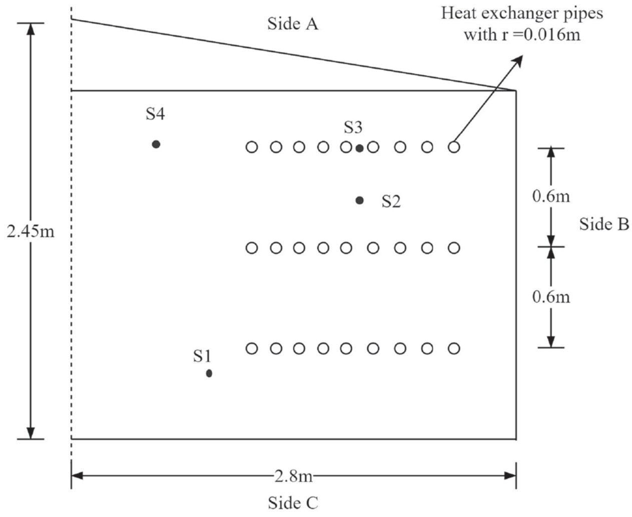

FIGURE 1: Axisymmetric two-dimensional geometry of the pile and with heat recovery pipes placed concentrically in the pile. S1(0.6, 1.0), S2(1.5, 1.8), S3(1.8, 1.8) and S4(2.0, 0.7) are the probes in the pile for measuring evolution of different variables, with coordinates indicating their depth distance from center.

2.2.4 Initial and Boundary Conditions

The initial conditions chosen for the model are described as,

$$T(t=0,x,y) = T_{ini}\ ;\ T_{air}(t=0,x,y) = \\ = T_{ini}\ ;\ O_2(t=0,x,y) = O_2^{amb}; \\ S(t=0,x,y) = S_o\ ;\ P(t=0,x,y) = P_{atm} \quad (15)$$

The initial temperature of the compost pile T_{ini} was the ambient temperature at the day of construction of the pile. S_o was calculated from the total amount of material used in the piles without water added to it. The model from Lukyanova considered the woodchips to be inert, in this model the wood degradation was also taken into consideration to calculate the initial substrate density. Separate boundary conditions were formulated for sides A and B (Figure 1) (eqn. 12), C (eqn. 13) and heat exchanger pipe walls (eqn.15). The images of the compost piles captured using the thermal camera clearly depict the higher temperature at the boundaries of the compost pile (Müller, 2017). Thus, heat loss at the boundary surfaces is described by Newton's law of cooling. The corresponding description for the following variables and the values for them are listed in Table 2 and 3. For sides A and B,

$$\frac{\partial T}{\partial \vec{n}}(t,\vec{x}) = -\frac{U_w}{C\quad \rho D}(T - T_{amb}) \quad (16)$$

$$\frac{\partial T}{\partial \vec{n}}(t,\vec{x}) = -\frac{U_g}{C\quad \rho D}(T - T_{gro}) \quad (17)$$

where $\vec{n}$ is an outward normal unit vector. The temperature of the ambient environment T_{amb} varied from -10.4°C to 37.8°C for the whole year ((CDC), DWD Climate Data Center). The ground temperature calculation for buildings is essential for heat loss balances. Therefore, for outdoor pilot scale composting reactors, the heat loss through the ground is also included (Thermal protection and energy economy in buildings - Part 6: Calculation of annual heat and energy use, 2003-01). The temperature T for this calculation was implemented from the experimental study.

$$T_{gro} = T_{amb} + f_g(T - T_{amb}) \quad (18)$$

For the heat exchanger boundary wall,

$$\frac{\partial T}{\partial \vec{n}}(t, \vec{x}) = -\frac{U_w}{C_{p,c}\rho D}(T - T_{pipe}) \quad (19)$$

For sides A and B, side C (ground) and heat exchanger pipe walls the boundary condition for air temperature was chosen respectively as,

$$T_{air}(t, \vec{x}) = T_{amb}; T_{air}(t, \vec{x}) = T_{gro}; T_{air}(t, \vec{x}) = T_{pipe} \quad (20)$$

For sides A and B, for oxygen concentration and pressure the following condition was chosen,

$$O_2(t, \vec{x}) = O_2^{amb} \,; P(t, \vec{x}) = P_{atm} \quad (21)$$

Since the ground is impermeable, a zero-flux condition was used at the base of the pile for oxygen concentration and pressure (eqn. 22). For the available substrate, all boundaries were impermeable (eqn. 23).

$$\frac{\partial O_2}{\partial \vec{n}} = 0; \frac{\partial P}{\partial \vec{n}} = 0 \quad (22)$$

$$\frac{\partial S}{\partial \vec{n}} = 0 \quad (23)$$

2.3 Simulation approach

Initially the model was simulated without the heat exchanger pipes in order to fit and validate the parameters to the data from the reference pile (Case Ref). After model validation, the heat exchanger pipes were incorporated into the pile geometry and five different case studies were simulated (Table 3).

2.3.1 Implementation in COMSOL

The partial differential module in COMSOL is used to find the solutions to the PDE (COMSOL Multiphysics® v. 5.3, 2019). The parameters, variables and functions were defined to account for the compaction effect and reaction rates (Table 2). The correction functions and the variation in the ambient temperature with time were integrated in the model using the analytic, interpolation and piecewise function feature available in the COMSOL working interface. An unstructured quad mesh was used, with a boundary layer meshing for the wall surfaces. The complete mesh consisted of 10387 elements. A time dependent study was designed for 200 days in 9 steps with 4 intervals of 15 days in which heat was recovered and other 5 intervals in which there was no heat extraction. The numerical solution of the equations was found using the implicit Backward Differentiation Formula solver.

3. RESULTS AND DISCUSSION

This section summarizes the model validation and the simulation results calculated from five different case studies.

3.1 Model validation

The model validation was carried out using the experimental data from the reference pile. The model could successfully predict the temperature development in the pile during the first 40 days of the composting process (Figure 2). The model also successfully predicted the temperature at different locations of the pile as well as the time taken to reach the peak temperature of 74°C in 55 to 75 days. The comparison of maximum temperatures from the experiment and the model only had a 3.8% difference despite the uncontrolled conditions during the experiment. The rise of temperature in the experiment after 160 days could be attributed to the effect of precipitation, which is a factor that this model did not consider. The model also predicts that the temperature remains above 55°C up to 200 days of simulation, similar to the experiment in which the temperature is above 55°C even after 315 days of composting (Schmidt-Baum, et al., 2020). The oxygen concentration profile is also in good agreement with observations made by Müller (Müller, 2017) and Schmidt-Baum et al. (Schmidt-Baum, et al., 2020), indicating the formation of an anaerobic region at the center of the pile. Substrate degradation could not be observed as the compost piles was still in operation. Nevertheless, the model showed good agreement with the study by Müller for temperature, oxygen concentration and substrate degradation (Müller, 2017).

3.2 Temperature

In the spatial profile, the initial phase of high temperatures in the outer portions (1.5m to 2.5m from origin) of the pile is due to oxygen availability at outer portions as compared to the inner portions of the pile (Figure 3). Once the sides of the piles are depleted, the higher temperature zone shifts towards the core of the pile indicating the degradation of the substrate remaining at the core of the compost

TABLE 3: Overview of the studies carried out using the model.

Case studies	[°C]	[°C]	[°C]	r [m]	Remarks
Case Ref	-	-10.6 to 16	$T_{amb} + f_g(T - T_{amb})$	-	Reference pile without heat extraction
Case 0	35	-10.6 to 16	$T_{amb} + f_g(T - T_{amb})$	0.016	Standard compost pile with heat extraction
Case I	35	-10.6 to 16	$T_{amb} + f_g(T - T_{amb})$	0.032	Doubled heat transfer area
Case II	30	-10.6 to 16	$T_{amb} + f_g(T - T_{amb})$	0.016	Lower pipe wall temperature
Case III	35	7.5 to 29.5	$T_{amb} + f_g(T - T_{amb})$	0.016	Warm period
Case IV	35	-10.6 to 16	Insulation	0.016	Ground insulation

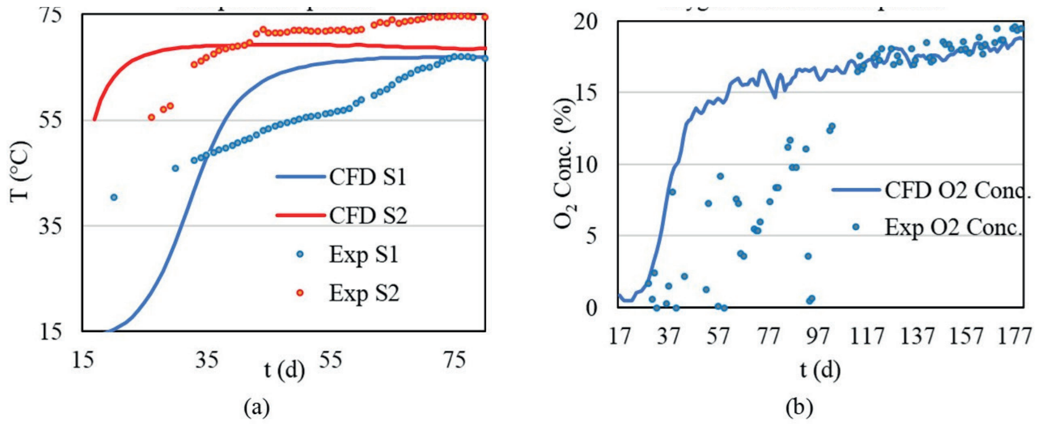

FIGURE 2: Profiles for experimental and CFD simulation: (a) Temperature and (b) Oxygen concentration.

pile, which is similar to the behaviour observed in the experiment by Müller and Schmidt-Baum et al. (Müller, 2017; Schmidt-Baum, et al., 2020). The temperature distribution around the pipe surfaces up to 0.05m was initially low. This is due to the lower amount of substrate available there for decomposition compared to other regions. However, almost all regions of the pile remained in the thermophilic (> 55 degrees C) stage from day 15 to 180 of composting. The middle layer of pipes remained at high temperatures as compared to the upper and lower pipe layers during the initial to final phases of the composting process due to lower heat loss to the atmosphere as compared to the upper pipe layer closer to the atmosphere and lower pipe layer closer to the ground. The temperature decreased during heat extraction and rose again when the heat extraction does not take place (Figure 4 (a)). The maximum temperature in the pile remained higher by more than 2°C for case IV. For all the cases, temperature near the base of the pile was less than 35°C during the first 35 days which shows the anaerobic degradation occurring on these days at the inner portions of the pile. In addition, for all the cases, the top layers of the pile were hotter, with differences of 5°C to

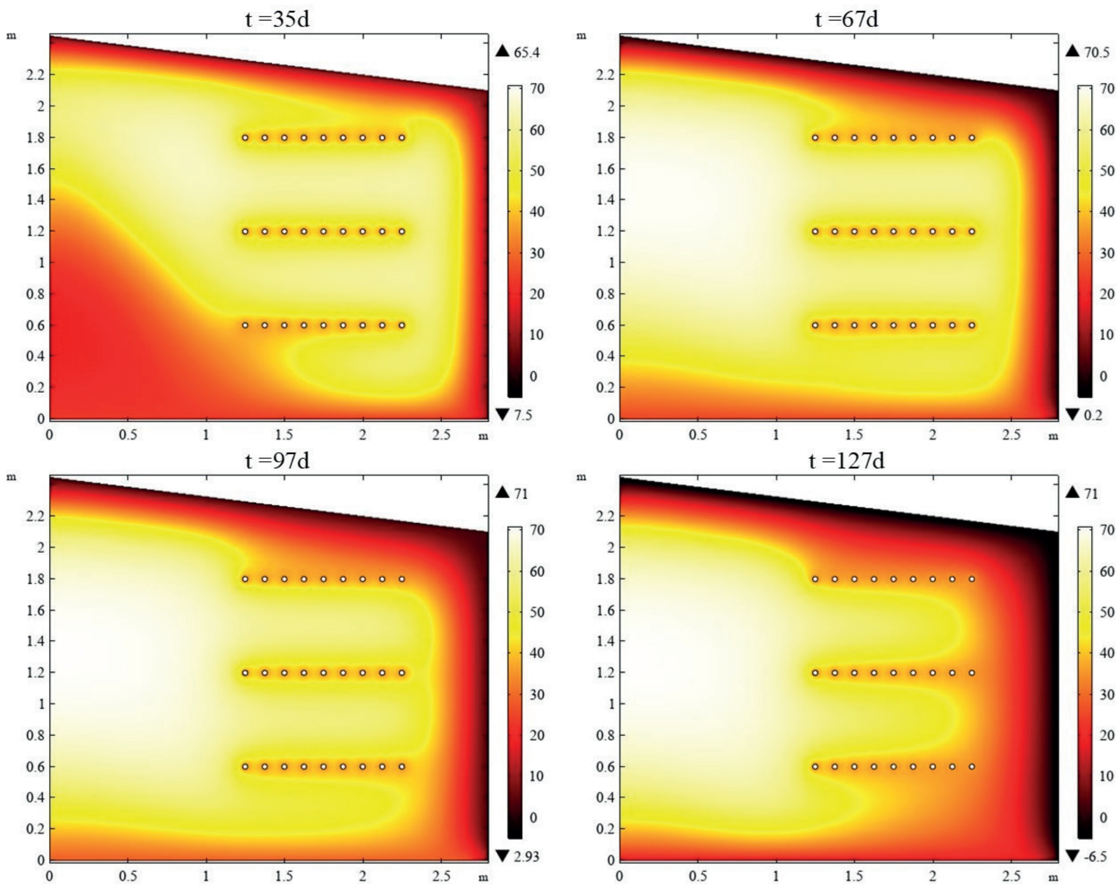

FIGURE 3: Spatial distribution of temperature for Case 0. Legend indicates the changes in T in °C.

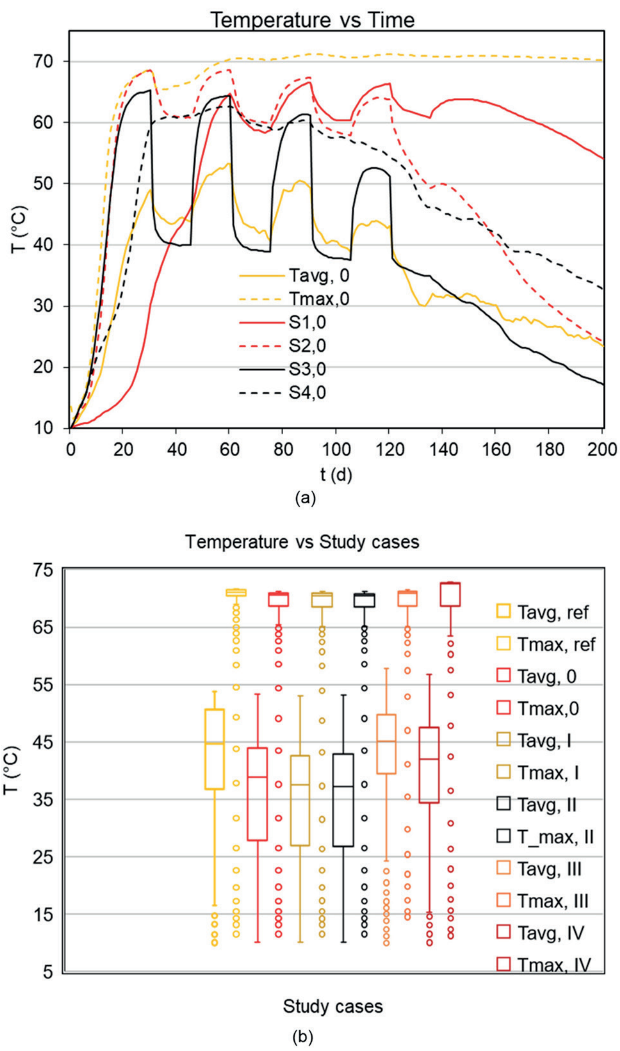

FIGURE 4: (a) Computed temperature data with time Tavg, 0 and Tmax, 0 indicate the average and maximum tempreature for Case 0 respectively. (b) Comparison of the average and maximum temperature for the different case studies.

the other regions during the first 30 days of the composting process.

Simulation studies show higher average temperature (45°C) and higher maximum temperature (71°C) in the reference pile indicating successful heat loss through heat extraction via heat exchanger compared to all other cases. For Case III and IV the average temperature remained above 35°C for 100 days. The maximum temperature varies among the case studies less than 0.1°C except for case III (Figure 4 (b)). The studies on the temperature profile for case I and case II indicated that the high temperature decreases in case of a higher heat exchanger surface area and lower pipe wall temperature. This decrease is due to the higher rate of heat extraction available to due to greater surface area. The temperature profile for case III depicts a difference of more than 2-10°C higher than Case 0; indicating that air entering the pile takes away less heat. The temperature was above 35°C even after 175 days in the simulation period which indicates comparatively lesser heat loss compared to case 0. The temperature distribution for case IV indicated higher temperatures at the base of the pile as compared to the pile without ground insulation. It indicates highest maximum temperature in the pile as compared to all other cases due to lower heat loss through the pile base. This indicates the need of insulation to reduce heat loss.

3.3 Oxygen

A qualitative comparison of the vertical profiles of the oxygen concentration in the pile indicates similar behaviour with the experimental case (Schmidt-Baum, et al., 2020) (Figure 5). The higher oxygen concentration at the walls is due to passive aeration through the walls of the compost pile. There are regions with oxygen concentration < 10% due to high degradation rate in the initial phase, which is mostly the upper part, or due to the insufficient aeration, which is the 0 - 1.5 m from the centre. When oxygen is not replenished it leads to anaerobic conditions and subsequently less heat production in this area. The oxygen concentration is available abundantly at the outer portion, which results in high degradation and high heat production at the outer regions, which is up to 0.8 m from the outer edge of the pile. The prediction of the oxygen profile thus matches exactly the behaviour observed by Müller (Müller, 2017). The oxygen concentration up to 0.2 m near the pipe walls decreases with heat extraction, which indicates that heat extraction enhances the decomposition process in these regions.

Comparing the probes in Case 0, all oxygen concentrations first drop to its lowest value at 0.5% on the 21st day due to the anaerobic conditions at probe S1 (Figure 6 (a)). The minimum oxygen concentration level in the whole pile on this day is 0.1% at different points, demonstrating anaerobic conditions. The probe S2 indicates an oxygen concentration greater than 15% at all times, due to passive aeration. The oxygen concentration recovers to ambient values after 120 days of simulation in the whole compost piles. The first initial drop in average oxygen concentration is the same for the Case Ref, Case 0, Case I and Case II since no heat recovery takes place and the other boundary conditions are the same (Figure 6 (b)). The average oxygen concentration was lower than 10.5% for Case III in the first 10 days of the composting process. Heat loss to the atmosphere and the ground is lower due to lower temperature gradient. Therefore, the compost pile remains in the thermophilic phase. Thus, the degradation rate is faster and higher oxygen consumption which results in more heat generation in different parts of the pile. The average oxygen concentration during the heat extraction process is at least 4% lower than compared to Case 0. This indicates that warmer inlet air temperature favours both heat production by oxygen consumption and lower heat loss to the atmosphere and the ground, due to the lower temperature gradient between the surroundings. Case IV has similar initial decrease in oxygen concentrations like Case III.

3.4 Substrate

Figure 7 indicates the formation of a highly degraded region at the outer section and a less degraded region at the inner portions, which is due to anaerobic conditions and lesser decomposition rate. In addition, there is also

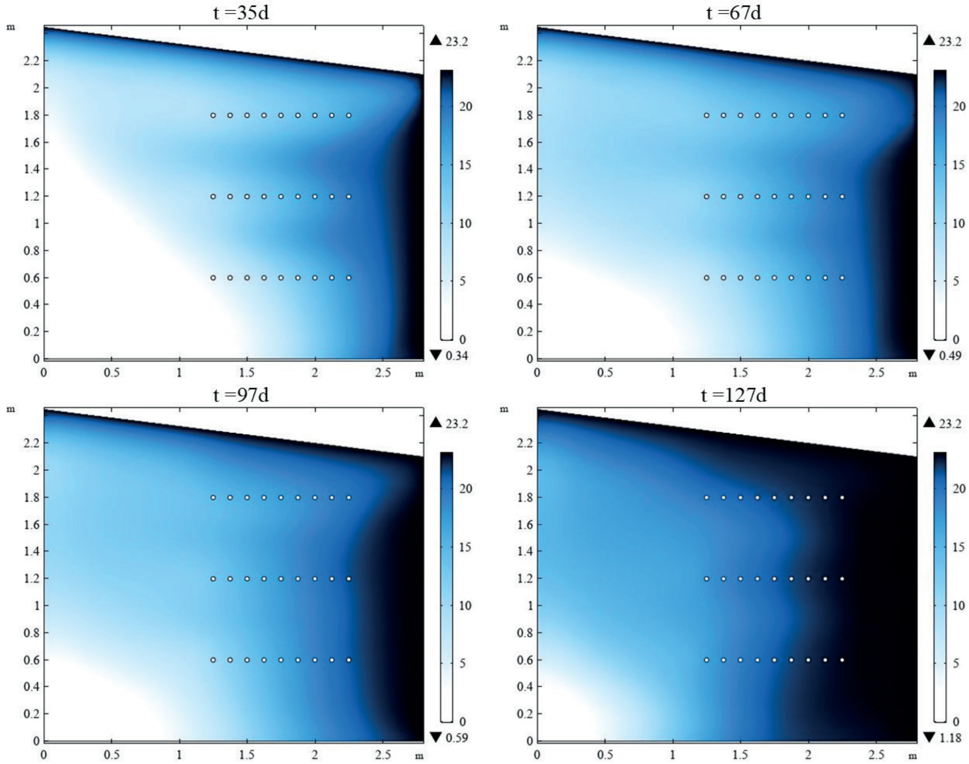

FIGURE 5: Spatial distribution of oxygen concentration (%) in the compost pile.

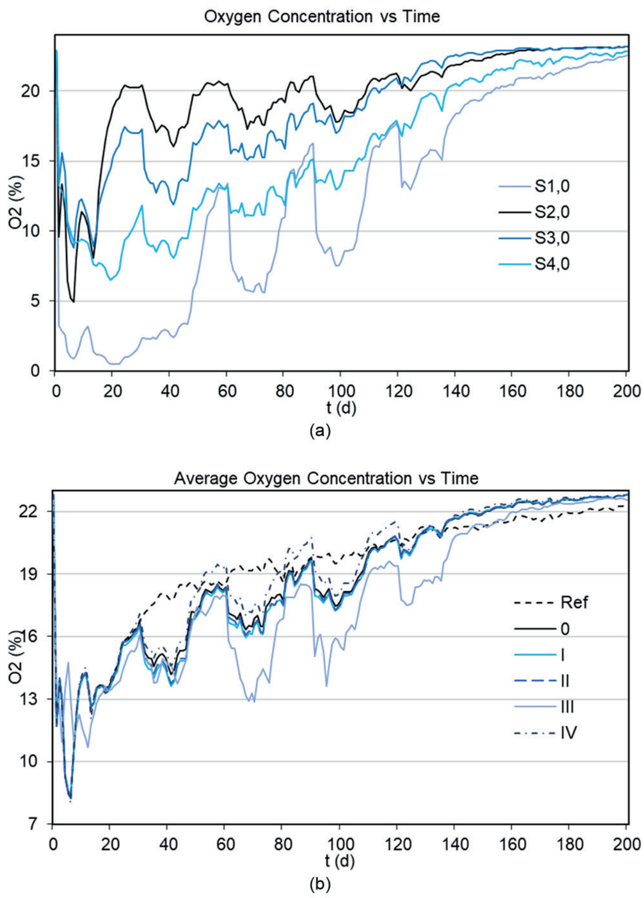

FIGURE 6: (a) Computed oxygen concentration data from probes with time; (ii) Computed average oxygen concentration profile (b) with time for different studies.

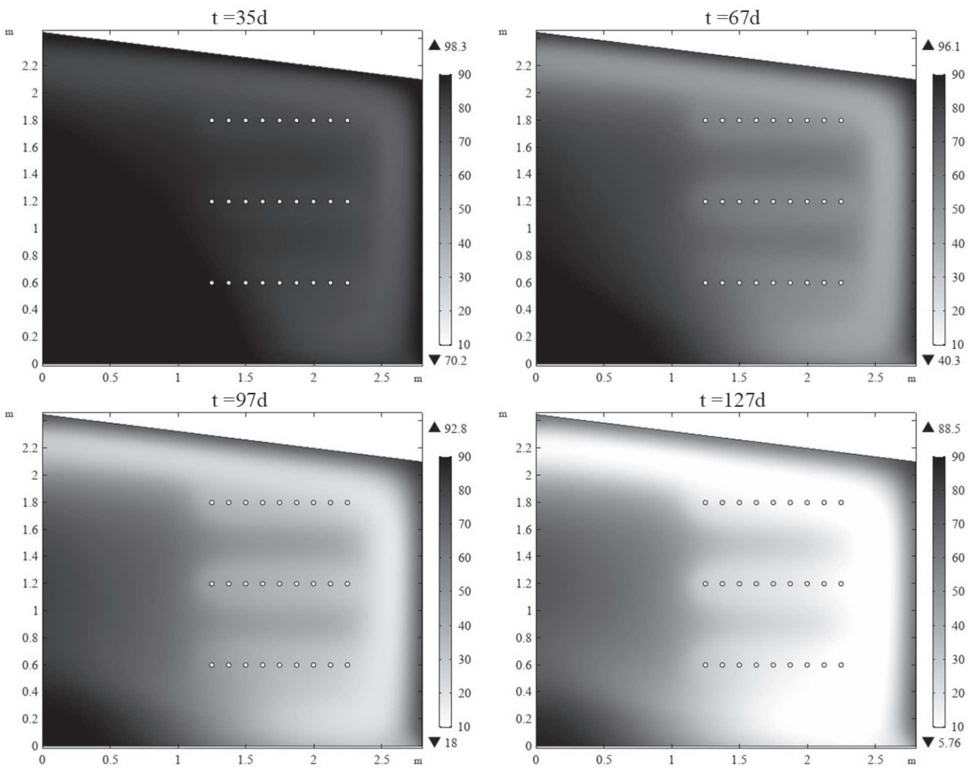

FIGURE 7: Spatial distribution of substrate concentration (%) in the compost pile.

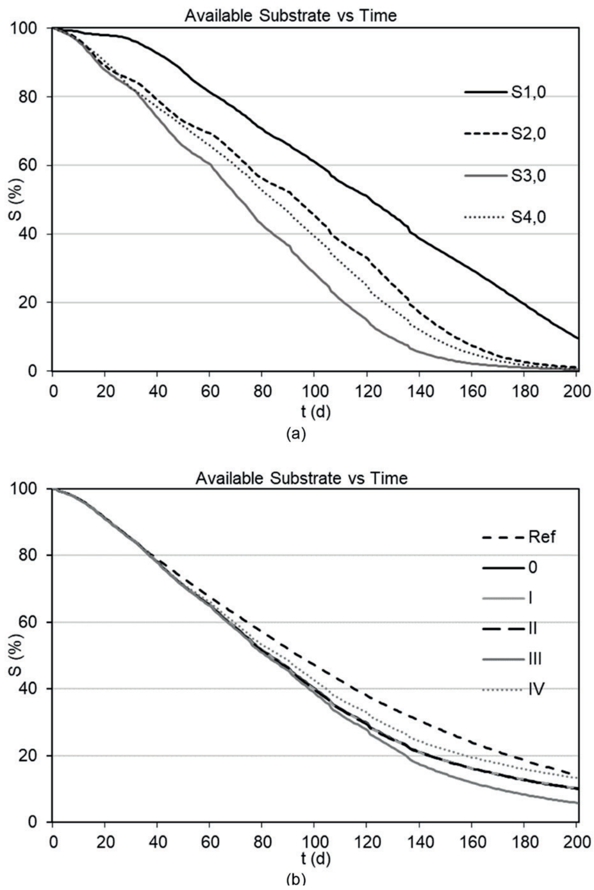

FIGURE 8: (a) Computed substrate concentration (%) data from probes with time (b) Computed average substrate degradation (%) with time.

a highly degraded region between 1.5 m and 2.7 m (from central axis) as concluded by experimental observations by Müller (Müller, 2017). During the process of heat extraction, substrate degradation varies slightly with heat extracted from the pile due to change in the composting phase at a lower temperature. On the 97th day of composting, there is a difference in degradation of around 30% (with respect to the total mass) near the pipe wall to 60% around (0.2 m above or below from the pipe wall like in oxygen concentration) despite the decrease in rate of degradation. The probe at the base of the compost pile depicts only 3.6% substrate degraded in the first 30 days, due to low temperature and low oxygen concentration. Nevertheless, after 200 days of simulation, the fraction of available substrate at all probes was less than 10%.

Probes show an initial phase of slow substrate degradation and increases degradation rate once temperature is higher than 55°C (Figure 8 (a)). For the case studies, there are differences up to 5% for available substrate (Figure 8 (b)). This leads to a slight decrease in degradation rate but do not affect the overall process. Case 0, I and II have the same profile of substrate degradation indicating heat recovery does not influence substrate degradation. In every case, at the base layer of the pile, degradation started after 25 days, indicating the low oxygen availability and lower temperature conditions at these piles that limits substrate degradation. Case III show accelerated degradation compared to the other cases since less heat is lost to the air. Case IV shows no accelerated degradation compared to the other cases despite lower heat loss through the ground. So, influence of convective heat loss on substrate degradation is higher than conductive heat loss.

3.5 Airflow pattern

The airflow pattern in the pile has an airflow less than $2x10^4$ m/s at the base of the pile due to higher density and lower porosity as a result of the compaction effects (Figure 9 (a)). The air velocities at the top portion of the pile could be attributed to high temperature and the lift of the air molecules due to buoyancy effects. The area with the highest airflow is the transition area as compared to the anaerobic core which is similar to the observations made by Müller (Müller, 2017; Schmidt-Baum, et al., 2020).

The airflow is strongest during heat extraction and with highest temperatures. The airflow distribution indicates, higher air velocity near the heat exchanger pipes that are closer to the outer regions of the pile during the heat extraction process. This effect is attributed to the buoyancy effects due to the movement of air as air gets heated up. This results in air rising and increasing the pressure around the pipe edges. This pushes the hot air away and sucking new air to the spaces between the heat exchanger pipes. The airflow pattern shows higher airflow up to 0.6 m (outer regions) like the pattern observed in the Case Ref. The airflow patterns in all study variations indicated only negligible variations of 3×10^{-5} m/s from one another. At the final stage of composting, slow air velocities were recorded in all cases.

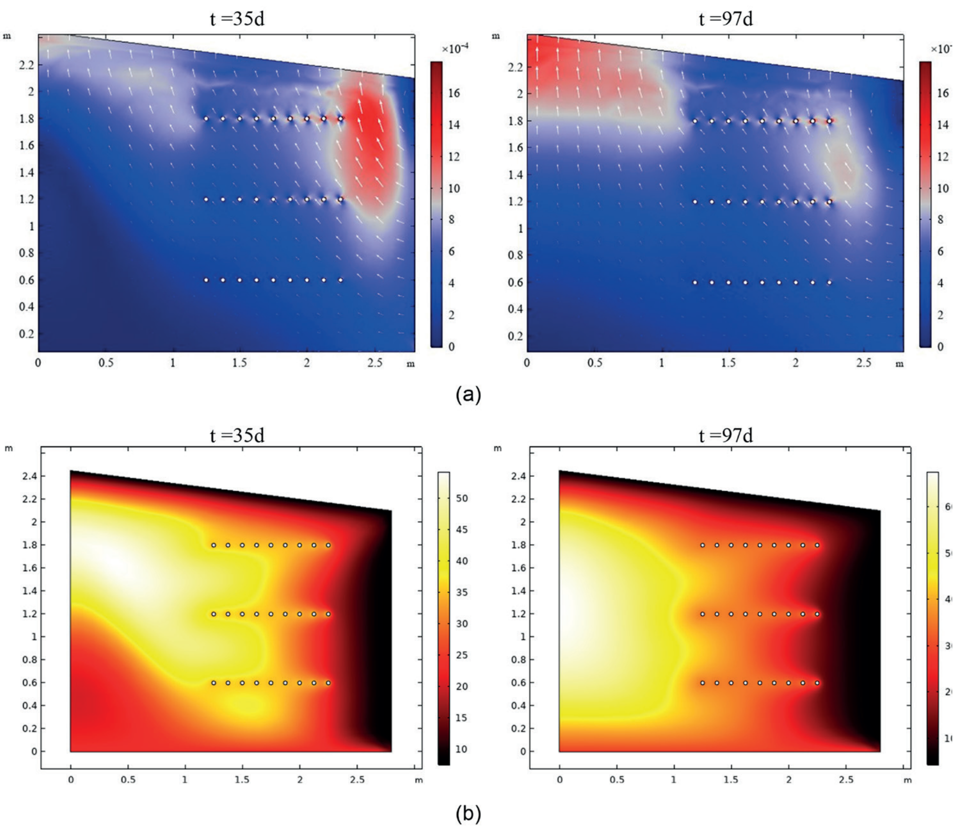

FIGURE 9: (a) Airflow patterns in the compost pile indicated by the arrows. The color legend indicates the air flow velocity in m/s (b) Spatial distribution of air temperature (°C) in the compost pile.

3.6 Air temperature

The air temperature profile in the pile shows higher air temperature towards inner portions as compared to outer portions (Figure 9 (b)). It indicates the convection of heat transfer from the compost material to the air and thereby resulting in the cooling of the compost pile. A temperature gradient of up to 20°C was observed which is not according to real experiment where air is saturated with water and represent solid phase temperature more closely. The air also transfers heat to the core of the compost pile thereby improving the degradation process at the core. Heat exchanger lowers air temperature due to heat recovering.

3.7 Heat extraction

The highest daily power output of 3 kW is on the first day of heat extraction (31st day) due to highest temperature gradient between the pipe wall and the compost pile temperature. The decreasing temperature gradient between the compost pile and the pipe wall is the reason for the decreasing power output. Afterwards, the 15 days recovery interval without heat recovery allows heat production so that the power output of the second phase is 2.5 kW. Intermitting, semi-continuous heat recovery is one operational behaviour confirmed by the simulation and experimental studies by Müller (Müller, 2017). Continuous heat extraction needs precise control based on exact heat production and has generally a lower temperature gradient for heat recovery. In all case studies, the amount of heat extracted decreases, due to the decreasing temperature difference between outer walls of the pipe and the compost pile temperature. 63% of the total power output is produced during the initial 75 days (Figure 10).

The percentage change in heat recovery is calculated by finding the increase in the total heat recovered from case 0 to each of the other four cases. Comparing average heat extraction for Case 0 and I show that 4% more heat can be extracted by double the pipe diameter, which indicates current pipe diameter of 0.016 m is sufficient for heat recovery. Furthermore, 10% more heat was recovered in Case II due to the higher temperature difference that exists between the compost pile and the pipe wall. Case III has the highest heat extraction of 11% of all cases. Cases III and IV indicate an 8% higher potential of heat extraction, because large portions of the pile remain at a higher temperature state due to the lower heat loss to the air or the ground. So, case IV demonstrated the importance of insulation for more power output.

The temperature profiles indicate possibly higher heat extraction rates with placing the pipes up to 0.2 m to the core to use the heat generated after 3 months of composting because temperature 0.2 m from the outer edges, have temperatures of 30°C after 70 days due to heat loss to atmosphere. Also, the degradation of the substrate at the core of pile even after 200 days of composting suggests that a greater heat extraction potential is available. This suggests that the current form of placing the pipes in 3 layers is effective for practical reasons but could be more optimised for greater heat recovery. Also heat from the core area would be available with passive aeration with methods like the dome aeration. Additionally, lowering pipe wall temperatures and increasing heat exchanger surface area would lead to more heat recovery.

4. CONCLUSIONS

This study successfully developed and demonstrated a spatial mathematical model for static outdoor compost piles with heat recovery. The comparison of the results from the experiment and the simulation predicted and explained the behaviour of the compost piles for temperature development, spatial distribution of oxygen concentration,

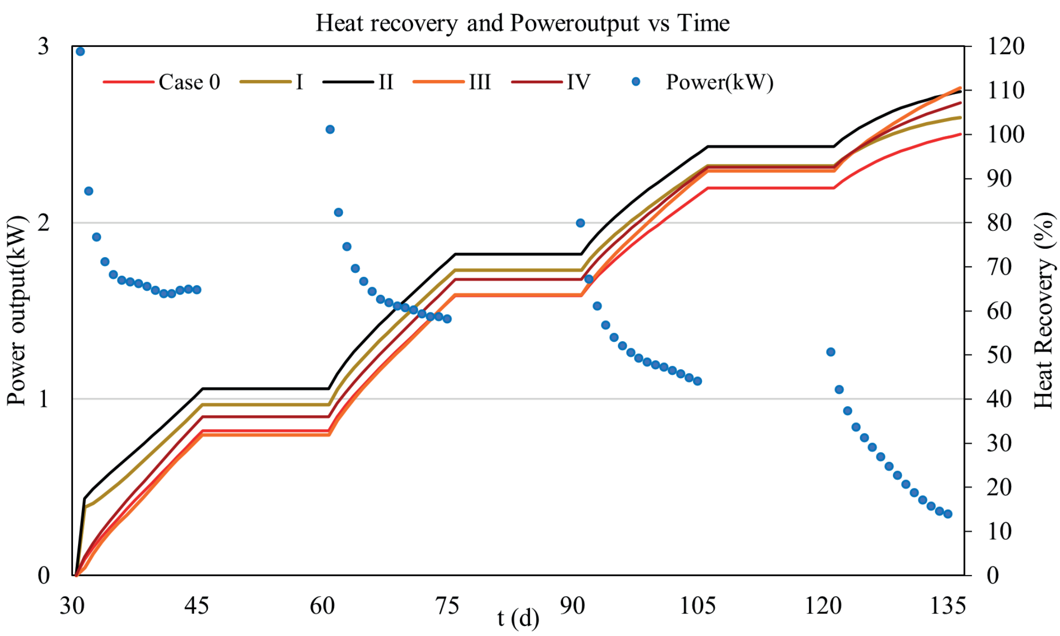

FIGURE 10: Comparison of Heat recovery (%) by the compost piles and power output for Case 0.

substrate degradation, airflow patterns and air temperature for 200 days. It confirmed that passive aeration is sufficient for an effective composting process in piles size 55 m^3 due to the chimney effect although the core area decomposes slower. The influence of heat extraction on a composting process became clear. The temperature and oxygen concentration in the pile decreases during heat extraction and it had minimal effects on the overall substrate degradation. Additional, intermittent heat extraction is preferred to improve the temperature gradient and thereby improves the power output from the piles. The sensitivity analysis via five case studies indicated that the walls including the base of the compost pile must be insulated to increase the power output from the compost piles. The power output obtained, indicates compost heating as a sustainable resident heating solution upon optimisation of the different parameters. This mathematical model could be used to study the interdependence of temperature, oxygen, substrate degradation and airflow to improve the power output from the heat exchanger and improve the composting process. In addition, the heat exchanger design and operational behaviour can be varied to achieve an optimum heat recovery rate. The parameters could be fitted more accurately only when the moisture effects, corresponding condensation and evaporation effects are accounted. Additional other passive aeration methods, like dome aeration, in combination with substrate variations can be examined. For this, this model must be further extended to incorporate external effects such as wind and precipitation to predict accurate data for different dependent variables.

AKNOWLEDGEMENTS

This research would not have been possible without the experimental work of the former student Sebastian Täschner and the advice of Dr. Torsten Schmidt-Baum, Tobias Hübner, Felix Bachnik and Daniel Dzofou Ngoumelah.

The project underlying this article was funded by the German Federal Ministry of Education and Research (BMBF) and carried out by the Deutsches Biomasseforschungszentrum (DBFZ) under grant number 031B0492A.

REFERENCES

(CDC), DWD Climate Data Center. (n.d.). Hourly station observations of air temperature at 2 m above ground in °C for Germany, version v19.3. Retrieved 10 10, 2019, from https://cdc.dwd.de/portal/

COMSOL Multiphysics® v. 5.3. (2019). Stockholm, Sweden: COMSOL AB. www.comsol.com

Das, K., & Keener, H. M. (1997, March 01). Moisture effect on compaction and permeability in composts. Journal of environmental engineering(3), pp. 275-281. https://doi.org/10.1061/(ASCE)0733-9372(1997)123:3(275)

Deipser, A. (2014). Prozesssimulation biologischer Abbauprozesse im Bereich der Abfallwirtschaft. Technische Universität Hamburg. Hamburg: Gesellschaft zur Förderung und Entwicklung der Umwelttechnologien an der Technischen Universität Hamburg-Harburg e.V. (GFEU). https://doi.org/10.15480/882.1181

European Environment Agency. (2017). Energy and mitigating climate change. Retrieved April 1, 2019, from https://www.eea.europa.eu/signals/signals-2017/infographics/energy-and-mitigating-climate-change/image/image_view_fullscreen

Finger, S. M., Hatch, R. T., & Regan, T. M. (1976). Aerobic microbial growth in semisolid matrices: heat and mass transfer limitation. Biotechnology and Bioengineering, 18(9), 1193-1218. doi:10.1002/bit.260180904

Hamelers, H. V. (2001). A mathematical model for composting kinetics. Wageningen University. Wageningen, Netherlands: Wageningen University. https://edepot.wur.nl/193815

Haug, R. T. (1993). The Practical Handbook of Compost Engineering. Boca Raton, Florida: CRC Press. https://doi.org/10.1201/9780203736234

Jaschke, N., & Schmidt-Baum, T. (2021). Heat Recovery of Compost Reactors: Field Study of Operational Behaviour, Heating Power and Influence Factors. Ecological Chemistry and Engineering, 28(2), 201-217. https://doi.org/10.2478/eces-2021-0015

Liang, Y., Leonard, J. J., Feddes, J. J., & McGill, W. B. (2004). A simulation model of ammonia volatilization in composting. Transactions of the ASAE(5), p. 1667.

Luangwilai, T., & Sidhu, H. (2010). Determining critical conditions for two dimensional compost piles with air flow via numerical simulations. ANZIAM Journal, 52, 463-481. doi:10.21914/anziamj.v52i0.3753

Luangwilai, T., S. Sidhu, H., & Nelson, M. I. (2012). Understanding the role of moisture in the self-heating process of compost piles. Chemeca 2012: Quality of life through chemical engineering: 23-26 September 2012. Wellington, New Zealand. Retrieved from https://ro.uow.edu.au/eispapers/196/

Luangwilai, T., Sidhu, H. S., & Nelson, M. I. (2018). One-dimensional spatial model for self-heating in compost piles: Investigating effects of moisture and air flow. Food and Bioproducts Processing, 108, 18-26. doi:10.1016/j.fbp.2017.12.001

Luangwilai, T., Sidhu, H. S., Nelson, M. I., & Chen, X. D. (2010). Modelling air flow and ambient temperature effects on the biological self-heating of compost piles. Asia-Pacific Journal of Chemical Engineering, 5(4), 609-618. https://doi.org/10.1002/apj.438

Luangwilai, T., Sidhu, H. S., Nelson, M. I., & Chen, X. D. (2010). Modelling air flow and ambient temperature effects on the biological self-heating of compost piles. Asia-Pacific Journal of Chemical Engineering, 5(4), 609-618. doi:10.1002/apj.438

Lukyanova, A. (2012). Spatial Modeling of the Composting Process. Edmonton, Alberta: University of Alberta. https://doi.org/10.7939/R3DN4065R

Malesani, R., Pivato, A., Bocchi, S., Lavagnolo, M. C., Muraro, S., & Schievano, A. (2021, May 1). Compost Heat Recovery Systems: An alternative to produce renewable heat and promoting ecosystem services. (Elsevier, Ed.) Environmental Challenges(4), p. 100131. https://doi.org/10.1016/j.envc.2021.100131

Mason, I. G. (2006). Mathematical modelling of the composting process: a review. Waste Management, 26(1), 3-21. doi:10.1016/j.wasman.2005.01.021

Mason, I. G. (2007). A Study of Power, Kinetics, and Modelling in the Composting Proces. Christchurch, New Zealand: University of Canterbury. doi:http://dx.doi.org/10.26021/2348

Mudhoo, A., & Mohee, R. (2008). Modeling Heat Loss during Self-Heating Composting Based on Combined Fluid Film Theory and Boundary Layer Concepts. Journal of Environmental informatics, 11(2).

Müller, N. (2017). Untersuchungen zum Betreibsverhalten von Biomeilern. Dresden: Technische Universität Dresden. http://d-nb.info/1227312180

Mwape, M. C., Muchilwa, I. E., Siagi, Z. O., & Yamba, F. D. (2020). Design and Performance Evaluation of a Hydronic Type Compost Heat Exchanger. Cogent Engineering, 7(1), 1846253. https://doi.org/10.1080/23311916.2020.1846253

Nwanze, K., & Clark, O. (2019). Optimizing Heat Extraction from Compost. Compost Science and Utilization, 27(4), 217-226. https://doi.org/10.1080/1065657X.2019.1686443

Rongfei, Z., Huiqing, G., & Wei, G. (2017). Comprehensive review of models and methods used for heat recovery from composting process. International Journal of Agricultural and Biological Engineering, 10(4), 1-12. doi:10.25165/j.ijabe.20171004.2292

Schmidt-Baum, T., Jaschke, N., Stinner, W., Schmidt, D., Windisch, F., Renner, D., & Pohl, R. (2020). IBÖM03: Entwicklung eines Mehrkammerbiomeilers zur effizienten Wärme und Komposterzeugung. Leipzig: DBFZ Deutsches Biomasseforschungszentrum gemeinnützige GmbH. https://doi.org/10.2314/KXP:176596945X

Sidhu, H. S., Nelson, M. I., & Chen, X. D. (2006). A simple spatial model for self-heating compost piles. ANZIAM Journal, 48, 135-150. doi:10.21914/anziamj.v48i0.86

Sidhu, H., Nelson, M. I., Luangwilai, T., & Chen, X. D. (2007). Mathematical modelling of the self-heating process in compost piles. Chemical Product and Process Modeling, 2(2), 8. doi:10.2202/1934-2659.1070

Thermal protection and energy economy in buildings - Part 6: Calculation of annual heat and energy use. (2003-01). German Institute for Standardisation. https://dx.doi.org/10.31030/9258155
Vidriales-Escobar, G., Rentería-Tamayo, R., Alatriste-Mondragón, F., & González-Ortega, O. (2017). Mathematical modeling of a composting process in a small-scale tubular bioreactor. Chemical Engineering Research and Design, I(20), 360-371. https://doi.org/10.1016/j.cherd.2017.02.006
Wikipedia. (2019, 01 18). Retrieved from Wikipedia: https://en.wikipedia.org/wiki/Density_of_air
Wikipedia. (2019, 01 18). Retrieved from https://en.wikipedia.org/wiki/Atmospheric_pressure
Yu, S. (2007). Heat and mass transfer in passively aerated compost. PhD thesis, University of Alberta, Alberta. https://doi.org/10.7939/r3-xd82-bk03
Zambra, C. E., Moraga, N. O., & Escudey, M. (2011). Heat and mass transfer in unsaturated porous media: Moisture effects in compost piles self-heating. International Journal of Heat and Mass Transfer, 54(13-14), 2801-2810. doi:10.1016/j.ijheatmasstransfer.2011.01.031
Zambra, C. E., Moraga, N. O., Rosales, C., & Lictevout, E. (2012). Unsteady 3D heat and mass transfer diffusion coupled with turbulent forced convection for compost piles with chemical and biological reactions. International Journal of Heat and Mass Transfer, 55(23-24), 6695-6704. doi:10.1016/j.ijheatmasstransfer.2012.06.078
Zampieri, P. (2017). Modelling of a technology for heat recovery from the composting process. Milan: Politecnico di Milano. Retrieved from https://www.politesi.polimi.it/handle/10589/141241